An engineered xCas12i with high activity, high specificity and broad PAM range

Hainan Zhang[1, 4], Xiangfeng Kong[1, 4], Mingxing Xue[1, 4], Zikang Wang[1, 4], Yinghui Wei[1, 4], Haoqiang Wang[1, 4], Jingxing Zhou[1], Weihong Zhang[1], Mengqiu Xu[1], Xiaowen Shen[1], Jinhui Li[1], Jing Hu[1], Na Zhong[1], Yingsi Zhou[1#], Hui Yang[1, 2, 3#]

[1] HUIEDIT Therapeutics Inc., Shanghai 200031, China.

[2] HUIGENE Therapeutics Inc., Shanghai 200131, China.

[3] Institute of Neuroscience, State Key Laboratory of Neuroscience, Key Laboratory of Primate Neurobiology, Center for Excellence in Brain Science and Intelligence Technology, Chinese Academy of Sciences, Shanghai 200031, China.

[4] These authors contributed equally to this work.

Correspondence to: ys@huiedit.com (Y.Z.), huiyang@huidagene.com (H.Y.)

Abstract

The type-V CRISPR effector Cas12i, with its smaller size, short crRNA guiding, and self-processing features, is a potentially versatile genome editing tool. By screening Cas12i proteins from a metagenomic database, we identified a natural variant with high activity in mammalian cells, named as xCas12i. We further engineered the PAM-interacting, REC, and RuvC domains for enhanced cleavage activity and specificity. This variant, named as high-fidelity Cas12Max, exhibited robust genome editing activity and minimal off-target activity with a broad 5'-TN recognition profile. With the fusion of deaminase TadA8e and further optimization of xCas12i, the base editor dCas12i-Tad8e also showed the high editing efficiency. This study provides highly efficient and specific tools for gene therapy.

Keywords: CRISPR, Cas12i, broad PAM recognition, dCas12i base editor

Introduction

The clustered regularly interspaced short palindromic repeats-Cas (CRISPR-Cas) systems, including type II Cas9 and type V Cas12 systems, which serve in the adaptive immunity of prokaryotes against viruses, have been developed into genome editing tools[1-3]. Compared with type II systems, the type V systems including V-A to V-K showed more functional diversity[4, 5]. Amongst them, Cas12i has a relatively smaller size (1033-1093 aa), compared to SpCas9 and Cas12a, and has a 5'-TTN protospacer adjacent motif (PAM) preference[4, 6, 7]. Cas12i is characterized by the capability of autonomously processing precursor crRNA (pre-crRNA) to form short mature crRNA. Cas12i mediates cleavage of dsDNA with a single RuvC domain, by preferentially nicking the non-target strand and then cutting the target strand[8-10]. These intrinsic features of Cas12i enable multiplex high-fidelity genome editing. However, the natural variants of Cas12i (Cas12i1 and Cas12i2), showed low editing efficiency which limits their utility for therapeutic gene editing.

To address these limitations, we screened ten natural Cas12i variants and found one, xCas12i, with robust high activity in HEK293T cells. Engineering of xCas12i by arginine substitutions at the PAM-interacting (PI), REC and RuvC domains led to the production of a variant, high-fidelity Cas12Max (hfCas12Max), with significantly elevated editing activity and minimal off-target cleavage efficiency. In addition, we assessed the base editing efficiency of xCas12i-based base editor, and thus expanded the genome-editing toolbox.

Results

Identification and characterization of type V-I systems xCas12i

In order to identify more Cas12i variants, we developed and employed a bioinformatics pipeline to annotate Cas12i proteins, CRISPR arrays and predicted PAM preferences, and found 10 new CRISPR/Cas12i systems. To evaluate the activity of these Cas12i variants in mammalian cells, we designed a fluorescent reporter system which detected the increased enhanced green fluorescent protein (EGFP) signal intensity activated by Cas-mediated dsDNA cleavage or double strand breaks (Fig.1a). This system relied on

56 the co-transfection of a plasmid coding for mCherry, a nuclear localization signal (NLS)
57 -tagged Cas protein and its guide RNA (gRNA) or crRNA, and one coding BFP and
58 activatable EGxxFP cassette, which is EGxx-target site-xxFP[11]. EGFP activation was
59 carried out by Cas mediated DSB and single-strand annealing (SSA)-mediated repair.
60 Using this system, we observed that a variant, xCas12i, with targeted crRNA induced
61 significant activation of EGFP expression (Fig. 1a, Fig. S1), and exhibited a higher editing
62 frequency than LbCas12a or SpCas9 as determined by Fluorescence Activated Cell
63 Sorter (FACS) analysis (Fig. 1b). The xCas12i variant was smaller in size compared to
64 SpCas9 and LbCas12a (Fig. 1c). Considering the 5'-TTN PAM preference of Cas12i, we
65 performed a NTTN PAM identification assay using the reporter system. We found that
66 xCas12i showed a consistent high frequency of EGFP activation at target sites with
67 5'-NTTN PAM sequences, while LbCas12a and SpCas9 had comparable activity at
68 5'-TTTN and 3'-NGG PAM, respectively (Fig. 1d).
69 To further confirm the dsDNA cleavage activity of xCas12i in mammalian cells, we
70 transfected an all-in-one plasmid encoding NLS tagged xCas12i with crRNAs targeting 37
71 sites from *TTR*[12], *PCSK9*[13] in HEK293T or *Ttr* in N2a cells. The editing efficiency, *i.e.* indel
72 (insertion and deletion) formation at these loci was measured 48 hours after transfection
73 using FACS and targeted deep sequencing (Fig. 1e). We found that xCas12i mediated a
74 high frequency, up to 90%, of indel formation at most sites from *Ttr*, *TTR* and *PCSK9*, with
75 a mean indel formation rate of over 50% (Fig. 1f-g). These data indicate that xCas12i
76 exhibits a robust genome editing efficiency in mammalian cells, suggesting it has
77 excellent potential for therapeutic genome editing applications.
78
79 **Engineered xCas12i mediates high-efficiency editing at 5'-TN PAM sites**
80 To enhance its activity and expand its scope of PAM site recognition, we sought to
81 engineer xCas12i protein via mutagenesis and screen for variants with higher efficiency
82 and broader PAM using a reporter system, similar to what is described above. Substitution
83 of an amino acid in the DNA-binding pocket with positively charged arginine (R) was
84 shown to enhance the activity of the type V system[14-16]. Combined with predictive
85 structural analysis of xCas12i, we performed an arginine scanning mutagenesis approach

86 in the PI, REC-I and RuvC-II domains, generating a library of over 500 mutants (Fig. 2a-b).
87 We then individually transfected these mutant variants with an activatable EGFP reporter
88 system in HEK293T cells and analyzed them by FACS (Fig. 2a). Based on the
89 fluorescence intensity of cells with activated EGFP, over 100 mutants showed an
90 increased frequency of activated cells relative to wild type (WT) xCas12i, and one mutant,
91 named as Cas12Max, containing N243R showed a 3.4-fold improvement (Fig. 2b). We
92 next targeted *DMD* or *Ttr* sites using the fluorescent reporter system, and found that
93 Cas12Max displayed a markedly increased frequency of EGFP activation, relative to WT
94 xCas12i (Fig. 2c, Fig. S2). To further test the efficacy of Cas12Max in targeting genomic
95 loci, we designed a total of eight gRNAs to target sites *TTR* and *PCSK9* in HEK293T cells
96 and three more targeting *Ttr* in N2a cells. Consistent with our previous result, Cas12Max
97 exhibited a significantly increased frequency of indels compared to WT xCas12i (Fig.
98 2d-e).
99 Additionally, to investigate Cas12Max's PAM preference, we performed a 5'-NNN PAM
100 recognition assay by designing reporter plasmids with the same target sequence but
101 different PAM. Besides showing a consistent or higher cleavage activity at sites with a
102 5'-TTN PAM, Cas12Max showed a similarly high cleavage activity for targets with TNN,
103 ATN, GTN and CTN PAM sites, compared with the commonly used Cas12[7, 17] (LbCas12a,
104 Ultra-AsCas12a) (Fig. 2f). Taken together, these results demonstrate that Cas12Max
105 exhibits high-efficiency editing activity with highly flexible 5'-TN or 5'-TNN PAM
106 recognition.
107
108 **hfCas12Max mediates high-efficient and specific genome editing**
109 To examine the specificity of Cas12Max, we transfected a construct designed to express it
110 with crRNA targeting *TTR*[12], and performed indel frequency analysis of on- and off-target
111 (OT) sites predicted by Cas-OFFinder[18]. Using reporter system or targeted deep
112 sequence analysis, we found that Cas12Max efficiently edited target sites and resulted in
113 significant indel formation at 2 of 3 predicted off-target sites (Fig. S3). To eliminate the
114 off-target activity of Cas12Max, we screened these mutants with mutations in the REC
115 and RuvC domains[19], which have undiminished on-target cleavage activity, for those with

116 no off-target activity, using two activatable reporter systems, each containing one OT site
117 (Fig. S4a). We found that four mutants (v4.1-V880R, v4.2-M923R, v4.3-D892R and
118 v4.4-G883R) maintained a high level of on-target editing activity and showed significantly
119 reduced off-target EGFP activation (Fig. S4b). We further combined these four amino acid
120 substitutions with N243R and/or E336R of Cas12Max and found that the variant v6.3
121 (N243R/D892R/G883R) showed the lowest off-target EGFP activation at OT.1 and OT.2
122 sites and high on-target at the ON.1 site (Fig. S4c-e). Targeted TIDE analysis of
123 endogenous TTR.2 site and its off-target sites in HEK293T showed that v6.3
124 (N243R/D892R/G883R) significantly reduced off-target indel frequencies at six OT sites
125 and retained on-target at ON site, compared to Cas12Max (Fig. 3a). In addition, relative to
126 Cas12Max (v1.1), v6.3 (N243R/D892R/G883R) retained comparable or even higher
127 on-target activity at DMD.1, DMD.2 and DMD.3 sties (Fig. S4f). Therefore, we named v6.3
128 as high-fidelity Cas12Max (hfCas12Max).
129 To comprehensively evaluate the performance of hfCas12Max in human cells, we
130 designed large number of target sites in the exons of *TTR* for various Cas nucleases. In
131 total, editing activity was monitored over 30 sites for hfCas12Max with TTN PAMs, 40 sites
132 for SpCas9 with NGG PAMs, 4 sites for LbCas12a with TTTN PAMs, 4 sites for Ultra
133 AsCas12a, and 7 sites for KKH-saCas9 with NNNRRT PAMs. Indel analysis showed that
134 hfCas12Max exhibited an average efficiency of 70%, higher activity than other Cas
135 nucleases, comparable activity with Cas12Max (Fig. 3b, Fig. S5a). Using 5'-NNN PAM
136 reporter system, hfCas12Max maintained the broad 5'-TN and 5'-TNN PAM recognition
137 profile similarly to Cas12Max (Fig. S5b). To further evaluate the specificity of hfCas12Max
138 in human cells, we determined indel frequencies of P2RX5 and NLRC4 on-target and their
139 corresponding *in silico* predicted off-target sites[20]. TIDE analysis showed that
140 hfCas12Max had a higher on-target editing efficiency and similarly almost no indel activity
141 at potential off target sites, compared to Ultra AsCas12a and LbCas12a (Fig. 3c-d).
142 Overall, these results demonstrate that hfCas12Max has high efficiency and specificity
143 and is superior to SpCas9 and other Cas12 nucleases.
144
145 **dxCas12i-based base editors efficiently mediate base editing in mammalian cells**

146 We further explored the base editing of xCas12i by generating a nuclease-deactivation
147 xCas12i (dxCas12i). This was done by first introducing single mutations (D650A, D700A,
148 E875A, or D1049A) in the conserved active site of xCas12i based on alignment to
149 Cas12i1[8] and Cas12i2[10] (Fig. S6a-b). Then, these variants were fused with TadA8e^{V106W}
150 or human APOBEC3A (hA3A^{W104A}) to form the dxCas12i base editors TadA8e.1-dxCas12i
151 and hA3A.1-dxCas12i, respectively[21-23]. The initial versions of TadA8e.1-dxCas12i and
152 hA3A.1-dxCas12i showed low base editing activity with frequencies of 8% A-to-G and 2%
153 C-to-T, respectively (Fig. 4b-d). To address this, we introduced single and combined
154 mutations for high cleavage activity into the PI and Rec domains of dxCas12i, which
155 resulted in significantly increased A-to-G editing activity. Among the improved variants,
156 dxCas12i-TadA8e-v2.2 (N243R/E336R) achieved 50% activity at A9 and A11 sites of the
157 *KLF4* locus, markedly higher than the 30% activity of dLbCpf1-TadA8e (Fig. 4b, Fig.
158 S7a-b). At target sites within *PCSK9*, TadA8e-dxCas12i-v2.2 showed a similarly increased
159 efficiency to mediate A-to-G transitions, higher than dLbCpf1-TadA8e (Fig. S8). We then
160 further engineered the NLS, linker, TadA8e protein and the N-terminus to produce
161 dxCas12i-TadA8e-v4.3 which exhibited a nearly 80% A-to-G editing efficiency, while the
162 editing activities of other dxCas12i-ABE versions were unchanged (Fig. 4c, Fig. S7c-d). In
163 addition, the substitution of dxCas12i-v1.2 (N243R) or dxCas12i-v2.2 (N243R/E336R)
164 showed consistently elevated C-to-T editing at C7 and C10 sites of *DYRK1A*, even higher
165 at C7 by dLbCpf1-hA3A (Fig. 4d). These results together demonstrate that engineered
166 dxCas12i-based editors exhibit the high base editing activity in mammalian cells.
167

168 **Discussion**

169 In this study, we demonstrate that the Type V-I Cas12i system enables versatile and
170 efficient genome editing in mammalian cells. We found a natural Cas12i variant, xCas12i,
171 that shows high editing efficiency at TTN-PAM sites. By semi-rational design and protein
172 engineering of its PI, REC, RuvC domains, we obtained a high-efficiency, high-fidelity
173 variant, hfCas12Max, which contains N243R, E336R, and D892R substitutions. In
174 agreement with the hypothesis that introducing arginine at key sites could strengthen the

175 binding between Cas and DNA, the introduction of N243R in the PI domain and E336R at
176 REC domain significantly increased editing activity and expanded PAM recognition.
177 Interestingly, D892R or G883R substitutions in the RuvC domain reduced off-target and
178 retained on-target cleavage activity, whereas alanine substitutions[24, 25], which has been
179 used to reduce off-target activity, did not. The D892R substituted hfCas12Max was
180 obviously more sensitive to mismatch, which suggests that D892R or G883R improved
181 sgRNA binding specificity. Our data suggests that a semi-rational engineering strategy
182 with arginine substitutions based on the EGFP-activated reporter system could be used
183 as a general approach to improve the activity of CRISPR editing tools.

184 Through engineering, our Cas12i system has achieved high editing activity, high
185 specificity and a broad PAM range, comparable to SpCas9, and better than other Cas12
186 systems. Given its smaller size, short crRNA guide, and self-processing features[4, 8, 10], the
187 Type V-I Cas12i system is suitable for *in vivo* multiplexed gene editing applications,
188 including AAV[26] or LNP[12, 13].

189 In addition, we have confirmed that the Type V-I Cas12i system can be used in base
190 editing applications. For base editor, the dCas12i system shows high A-to-G editing at
191 A9-A11 sites even A19 of KLF locus, and C-to-T editing at A7-A10 sites, which is similar to
192 the dCas12a system but is distinct from the dCas9/nCas9 system. Comparable to
193 dCas12a, dCas12i-BE exhibited higher base editing activity at KLF4, PCSK9 and
194 DYRK1A loci (Fig. 4c-d), suggesting it may have more potential as a base editor. This
195 suggests that the dCas12i system is useful for broad genome engineering applications,
196 including epigenome editing, genome activation, and [1, 27-30].

197 In summary, the Cas12i system described here, which has robust editing activity and
198 high specificity, is a versatile platform for genome editing or base editing in mammalian
199 cells and could be useful in the future for *in vivo* or *ex vivo* therapeutic applications.

200

201 **Material and methods**

202 **Plasmid vector construction.**

203 Human codon-optimized *Cas12i*, *TadA8e* and human *APOBEC3A* genes were

204 synthesized by the GenScript Co., Ltd., and cloned to generate
205 pCAG_NLS-Cas12i-NLS_pA_pU6_BpiI_pCMV_mCherry_pA by Gibson Assembly. crRNA
206 oligos were synthesized by HuaGene Co., Ltd., annealed and ligated into *BpiI* site to
207 produce the pCAG_NLS-Cas12i-NLS_pA_pU6_crRNA_pCMV_mCherry_pA.
208

209 **Cell culture, transfection and flow cytometry analysis.**

210 The mammalian cell lines used in this study were HEK293T and N2A. Cells were cultured
211 in Dulbecco's modified Eagle's medium (DMEM) supplemented with 10% FBS,
212 penicillin/streptomycin and GlutMAX. Transfections were performed using Polyetherimide
213 (PEI). For variant screening, HEK293T cells were cultured in 24-well plates, and after 12
214 hours 2 μg of the plasmids (1 μg Cas12i of a mutant plasmid and 1 μg of the reporter
215 plasmid) were transfected into these cells with 4 μL PEI. 48 hours after transfection,
216 mCherry and EGFP fluorescence were analyzed using a Beckman CytoFlex
217 flow-cytometer. For assay of mutations in target sites of endogenous genes, 1 μg plasmid
218 with Cas12i targeting crRNA was transfected into HEK293T or N2A cells, which were then
219 sorted using a BD FACS Aria III, BD LSRFortessa X-20 flow cytometer, 48 hours after
220 transfection.
221

222 **Detection of gene editing frequency.**

223 Six thousand sorted cells were lysed in 20 μl of lysis buffer (Vazyme). Targeted sequence
224 primers were synthesized and used in nested PCR amplification by Phanta Max
225 Super-Fidelity DNA Polymerase (Vazyme). TIDE and targeted deep sequence analysis
226 was used to determine indel frequencies. Sanger sequencing and EditR were used for
227 quantification of base substitutions (A-to-G or C-to-T).
228

229 **Acknowledgements**

230 This work was supported by HUIEDIT Therapeutics Inc. We kindly thank Yuan Yuan, IP &
231 Legal Director from HUIGENE Therapeutics Inc., for helpful discussion.
232

Authors' Contributions

H.Z., and Y.Z. jointly conceived and designed the project. H.Z., H.W., J.Z., W.Z., M.X., and X.K., performed experiments with plasmid construction, cell culture and FACS and data analysis. M.X., Z.W., Y.W., X.S., J.L., J.H., and N.Z. assisted with experiments. H.Y. supervised the whole project. H.Z., Y.Z., and H.Y. wrote and revised the manuscript.

Conflict of interest

The authors disclose a patent application relating to aspects of this work. Y.Z. and H.Y. is the founder of HUIEDIT Therapeutics Inc., and H.Y. is also the founder of HUIGENE Therapeutics Inc.

Reference

1. Anzalone, A.V., Koblan, L.W. & Liu, D.R. Genome editing with CRISPR-Cas nucleases, base editors, transposases and prime editors. *Nat Biotechnol* **38**, 824-844 (2020).
2. Doudna, J.A. The promise and challenge of therapeutic genome editing. *Nature* **578**, 229-236 (2020).
3. Makarova, K.S. et al. Evolutionary classification of CRISPR-Cas systems: a burst of class 2 and derived variants. *Nat Rev Microbiol* **18**, 67-83 (2020).
4. Yan, W.X. et al. Functionally diverse type V CRISPR-Cas systems. *Science* **363**, 88-91 (2019).
5. Kleinstiver, B.P. et al. Genome-wide specificities of CRISPR-Cas Cpf1 nucleases in human cells. *Nature Biotechnology* **34**, 869-+ (2016).
6. Cong, L. et al. Multiplex Genome Engineering Using CRISPR/Cas Systems. *Science* **339**, 819-823 (2013).
7. Zetsche, B. et al. Cpf1 is a single RNA-guided endonuclease of a class 2 CRISPR-Cas system. *Cell* **163**, 759-771 (2015).
8. Zhang, B. et al. Mechanistic insights into the R-loop formation and cleavage in CRISPR-Cas12i1. *Nature communications* **12**, 3476 (2021).
9. Zhang, H., Li, Z., Xiao, R. & Chang, L. Mechanisms for target recognition and cleavage by the Cas12i RNA-guided endonuclease. *Nat Struct Mol Biol* **27**, 1069-1076 (2020).
10. Huang, X. et al. Structural basis for two metal-ion catalysis of DNA cleavage by Cas12i2. *Nature communications* **11**, 5241 (2020).
11. Yang, Y. et al. Highly Efficient and Rapid Detection of the Cleavage Activity of Cas9/gRNA via a Fluorescent Reporter. *Appl Biochem Biotechnol* **180**, 655-667 (2016).

269 12. Gillmore, J.D. et al. CRISPR-Cas9 In Vivo Gene Editing for Transthyretin Amyloidosis.
270 *The New England journal of medicine* **385**, 493-502 (2021).
271 13. Musunuru, K. et al. In vivo CRISPR base editing of PCSK9 durably lowers cholesterol
272 in primates. *Nature* **593**, 429-434 (2021).
273 14. Strecker, J. et al. Engineering of CRISPR-Cas12b for human genome editing. *Nature*
274 *communications* **10**, 212 (2019).
275 15. Kleinstiver, B.P. et al. Engineered CRISPR-Cas12a variants with increased activities
276 and improved targeting ranges for gene, epigenetic and base editing. *Nat Biotechnol*
277 **37**, 276-282 (2019).
278 16. Xu, X. et al. Engineered miniature CRISPR-Cas system for mammalian genome
279 regulation and editing. *Mol Cell* **81**, 4333-4345 e4334 (2021).
280 17. Zhang, L. et al. AsCas12a ultra nuclease facilitates the rapid generation of therapeutic
281 cell medicines. *Nature communications* **12**, 3908 (2021).
282 18. Bae, S., Park, J. & Kim, J.S. Cas-OFFinder: a fast and versatile algorithm that
283 searches for potential off-target sites of Cas9 RNA-guided endonucleases.
284 *Bioinformatics* **30**, 1473-1475 (2014).
285 19. Yuen, C.T.L. et al. High-fidelity KKH variant of Staphylococcus aureus Cas9 nucleases
286 with improved base mismatch discrimination. *Nucleic Acids Res* **50**, 1650-1660
287 (2022).
288 20. Kim, D.Y. et al. Efficient CRISPR editing with a hypercompact Cas12f1 and
289 engineered guide RNAs delivered by adeno-associated virus. *Nat Biotechnol* **40**,
290 94-102 (2022).
291 21. Wang, X. et al. Cas12a Base Editors Induce Efficient and Specific Editing with Low
292 DNA Damage Response. *Cell Rep* **31**, 107723 (2020).
293 22. Richter, M.F. et al. Phage-assisted evolution of an adenine base editor with improved
294 Cas domain compatibility and activity. *Nat Biotechnol* **38**, 883-891 (2020).
295 23. Li, X. et al. Base editing with a Cpf1-cytidine deaminase fusion. *Nat Biotechnol* **36**,
296 324-327 (2018).
297 24. Bravo, J.P.K. et al. Structural basis for mismatch surveillance by CRISPR-Cas9.
298 *Nature* **603**, 343-347 (2022).
299 25. Kleinstiver, B.P. et al. High-fidelity CRISPR-Cas9 nucleases with no detectable
300 genome-wide off-target effects. *Nature* **529**, 490-495 (2016).
301 26. Wang, D., Zhang, F. & Gao, G. CRISPR-Based Therapeutic Genome Editing:
302 Strategies and In Vivo Delivery by AAV Vectors. *Cell* **181**, 136-150 (2020).
303 27. Wang, H. et al. CRISPR-Mediated Programmable 3D Genome Positioning and
304 Nuclear Organization. *Cell* **175**, 1405-1417 e1414 (2018).
305 28. Konermann, S. et al. Genome-scale transcriptional activation by an engineered
306 CRISPR-Cas9 complex. *Nature* **517**, 583-588 (2015).
307 29. Nakamura, M., Gao, Y., Dominguez, A.A. & Qi, L.S. CRISPR technologies for precise
308 epigenome editing. *Nat Cell Biol* **23**, 11-22 (2021).
309 30. Fellmann, C., Gowen, B.G., Lin, P.C., Doudna, J.A. & Corn, J.E. Cornerstones of
310 CRISPR-Cas in drug discovery and therapy. *Nat Rev Drug Discov* **16**, 89-100 (2017).

311

312 **Figure Legends**

313 **Fig.1 Identification and characterization of type V-I systems. a,** Transfection of
314 plasmids coding Cas12i and sgRNA activates EGFP. **b,** xCas12i mediated EGFP
315 activation efficiency determined by flow cytometry. **c,** Nuclease domain organization of
316 SpCas9, LbCas12a, and xCas12i. **d,** PAM scope comparison of xCas12i, LbCas12a,
317 SpCas9. xCas12i exhibits a higher editing efficiency at 5'-TTN PAM than Cas12a, and a
318 comparable editing efficiency to SpCas9. **e,** Flow diagram for detection of genome editing
319 efficiency by transfection of an all-in-one plasmid containing xCas12i and targeted gRNA
320 into HEK293T cells, followed by FACS and NGS analysis. **f-g,** xCas12i mediates robust
321 genome editing (up to 90%) at the *Ttr* locus in N2a cells and at the *TTR* and *PCSK9* loci in
322 HEK293T cells.
323
324 **Fig.2 Cas12Max mediates high-efficiency editing and expands its PAM recognition.**
325 **a,** Schematics of protein engineering strategy using an activatable EGFP reporter
326 screening system. **b,** The relative editing frequencies of over 500 rationally engineered
327 Cas12Max mutants. **c-e,** Cas12Max exhibits significantly increased cleavage activity than
328 WT at various genomic or reporter plasmids target sites. **f,** Cas12Max exhibits a broader
329 PAM recognition profile than LbCas12a, including 5'TN- and 5'TNN- PAM.
330
331 **Fig.3 hfCas12Max mediates high-efficient and -specific editing. a,** TIDE analysis
332 shows that Cas12Max-v6.3 (hfCas12Max) retains comparable activity at TTR.2-ON
333 targets and almost no at 6 OT sites, to Cas12Max. **b,** Comparison of indel activity from
334 Cas12Max, hfCas12Max, LbCas12a, Ultra AsCas12a, SpCas9 and KKH-saCas9 at TTR
335 locus. hfCas12Max retains comparable activity of Cas12Max, and higher gene-editing
336 efficiency than other Cas proteins. Each dot represents one of three repeats of single
337 target site. **c-d,** Off-target efficiency of hfCas12Max, LbCas12a, and Ultra-AsCas12f at
338 in-silico predicted off-target sites, determined by targeted deep sequencing. Sequences of
339 on-target and predicted off-target sites are shown, PAM sequences are in blue and
340 mismatched bases are in red.
341
342 **Fig.4 dCas12Max-TadA8e and dCas12Max-hA3A.1 mediated high base editing**

343 **activity. a**, Schematics of different versions of dCas12Max BEs. **b**, The A-to-G editing
344 activity of TadA8e.1-dxCas12i-v2.2 was largely increased by combining v1.2 and v1.3
345 variant. **c**, Comparison of A-to-G editing frequency at the KLKF4 site from
346 TadA8e.1-dxCas12i-v1.2, v2.2 and v4.3, ABE-dCas12Max (TadA8e-dxCas12i-v4.3)
347 shows a high editing activity of 80%. **d**, Comparison of C-to-T editing frequency at the
348 DYRK1A site from hA3A.1-dxCas12i, -v1.2 and v2.2, CBE-dCas12Max
349 (hA3A.1-dxCas12i-v2.2) shows a high editing activity of 50%.

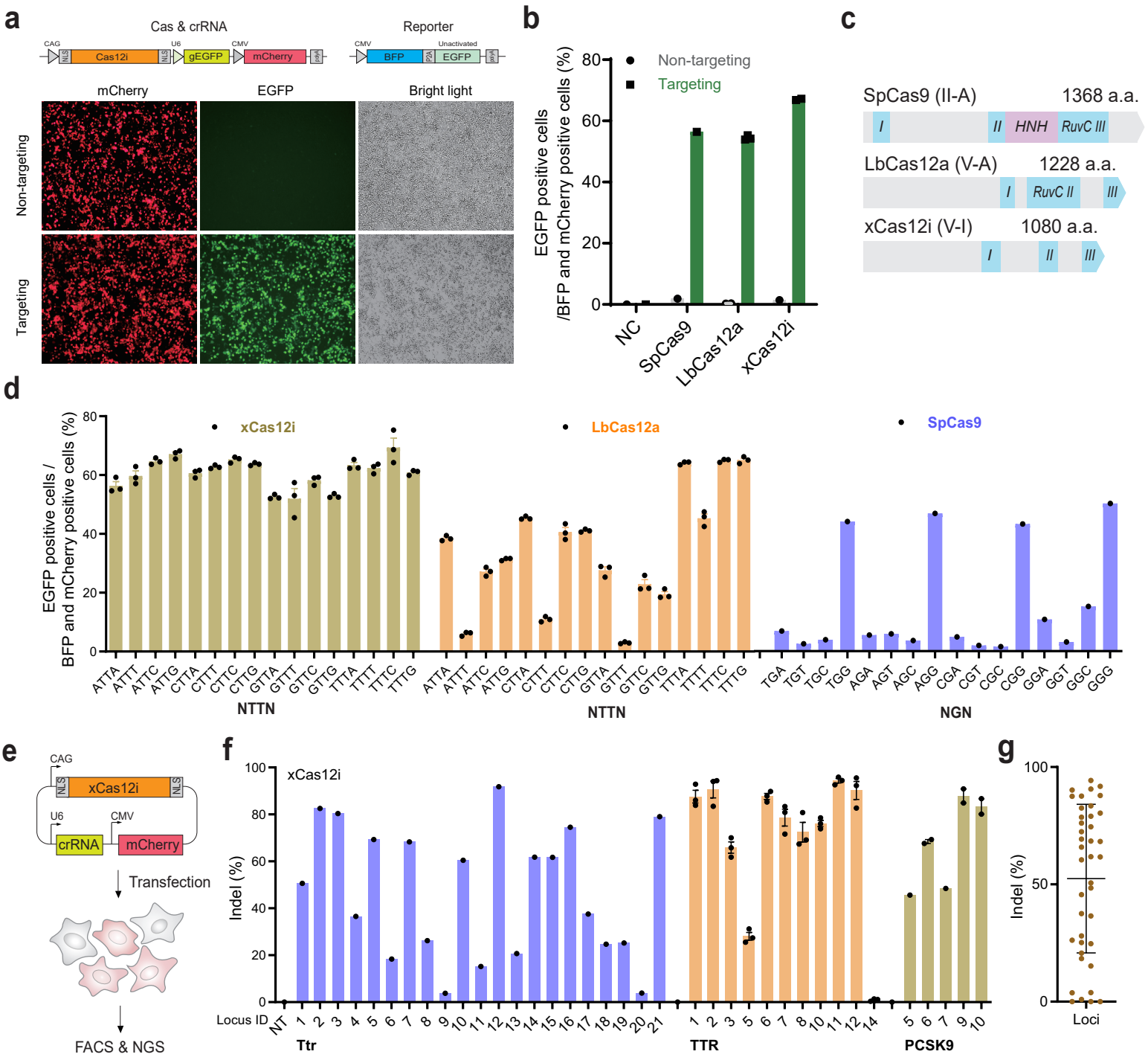

Fig.1 Identification and characterization of type V-I systems. a, Transfection of plasmids coding Cas12i and sgRNA activates EGFP. **b**, xCas12i mediated EGFP activation efficiency determined by flow cytometry. **c**, Nuclease domain organization of SpCas9, LbCas12a, and xCas12i. **d**, PAM scope comparison of xCas12i, LbCas12a, SpCas9. xCas12i exhibits a higher editing efficiency at 5'-TTN PAM than Cas12a, and a comparable editing efficiency to SpCas9. **e**, Flow diagram for detection of genome editing efficiency by transfection of an all-in-one plasmid containing xCas12i and targeted gRNA into HEK293T cells, followed by FACS and NGS analysis. **f-g**, xCas12i mediates robust genome editing (up to 90%) at the Ttr locus in N2a cells and at the TTR and PCSK9 loci in HEK293T cells.

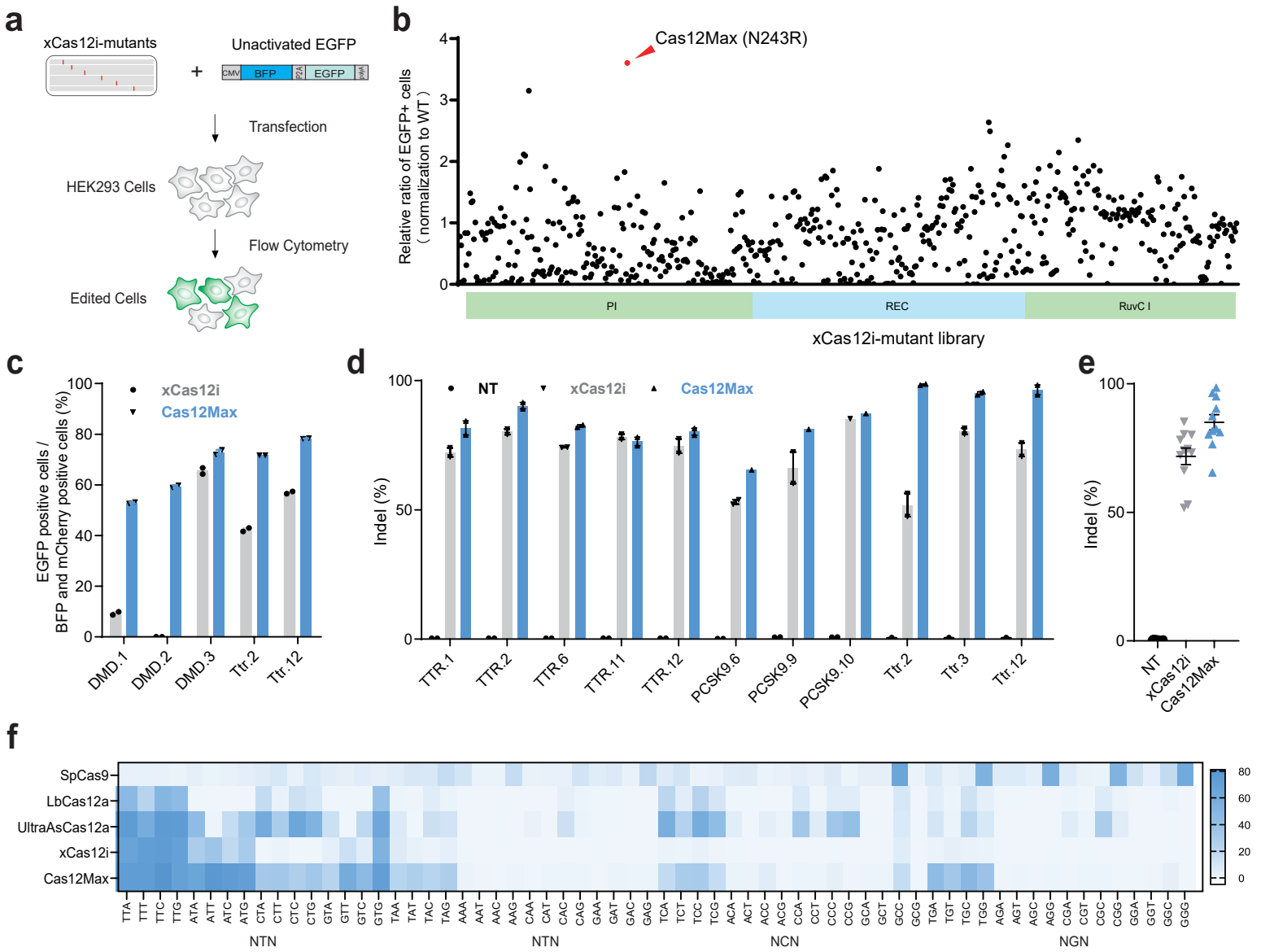

Fig.2 Cas12Max mediates high-efficiency editing activity and expand 5'TN-PAM scope. a, Schematics of protein engineering strategy using an activatable EGFP reporter screening system. **b**, The relative editing frequencies of over 500 rationally engineered Cas12Max mutants. **c-e**, Cas12Max exhibits significantly increased cleavage activity than WT at various genomic or reporter plasmids target sites. **f**, Cas12Max exhibits a broader PAM recognition profile than LbCas12a, including 5'TN- and 5'TNN- PAM.

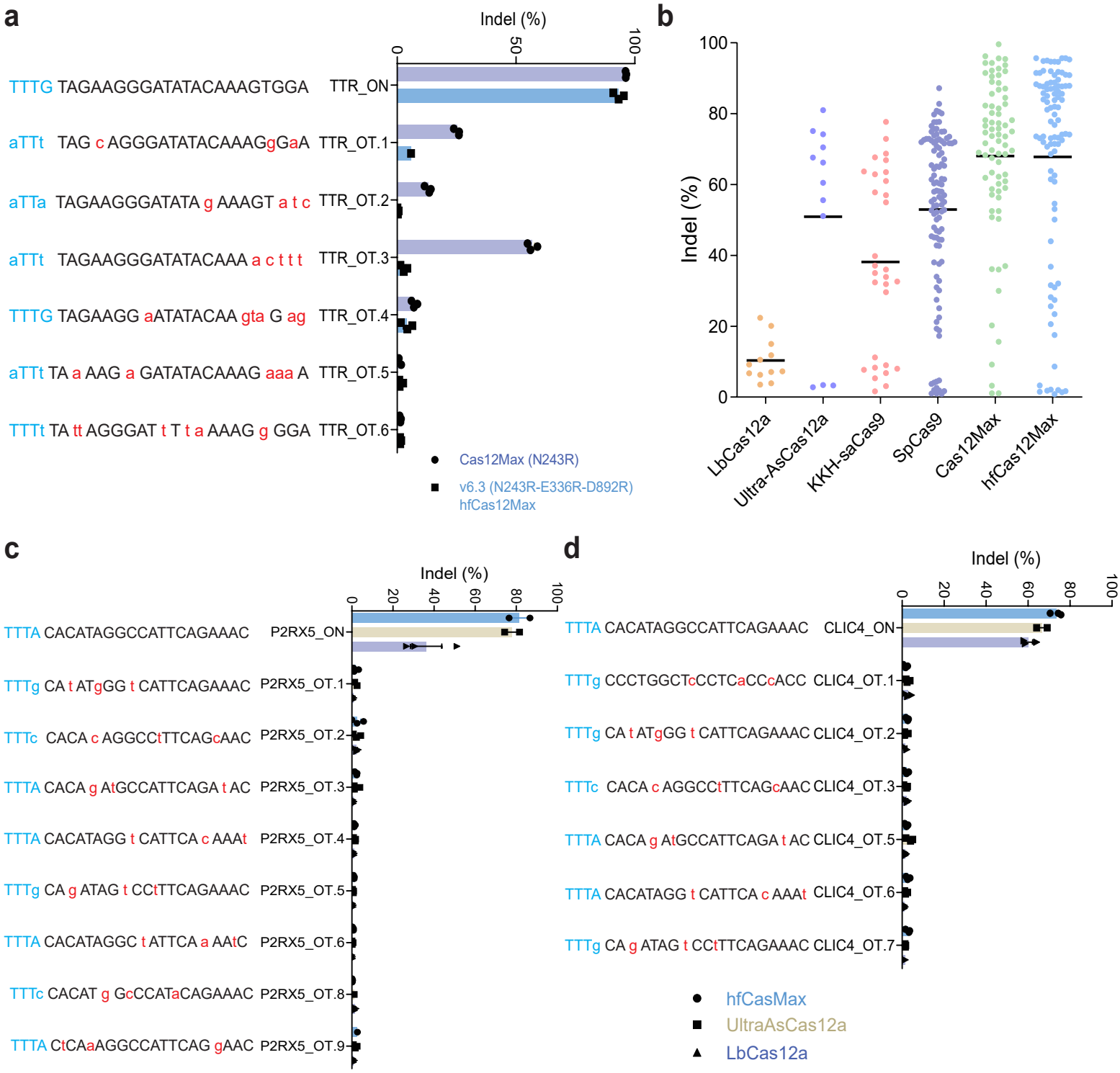

Fig.3 hfCas12Max mediates high-efficient and -specific editing. a, TIDE analysis shows that Cas12-Max-v6.3 (hfCas12Max) retains comparable activity at TTR.2-ON targets and almost no at 6 OT sites, to Cas12Max. **b**, Comparison of indel activity from Cas12Max, hfCas12Max, LbCas12a, Ultra AsCas12a, SpCas9 and KKH-saCas9 at TTR locus. hfCas12Max retains comparable activity of Cas12Max, and higher gene-editing efficiency than other Cas proteins. Each dot represents single target site. **c-d**, Off-target efficiency of hfCas12Max, LbCas12a, and Ultra-AsCas12f at *in-silico* predicted off-target sites, determined by targeted deep sequencing. Sequences of on-target and predicted off-target sites are shown, PAM sequences are in blue and mismatched bases are in red.

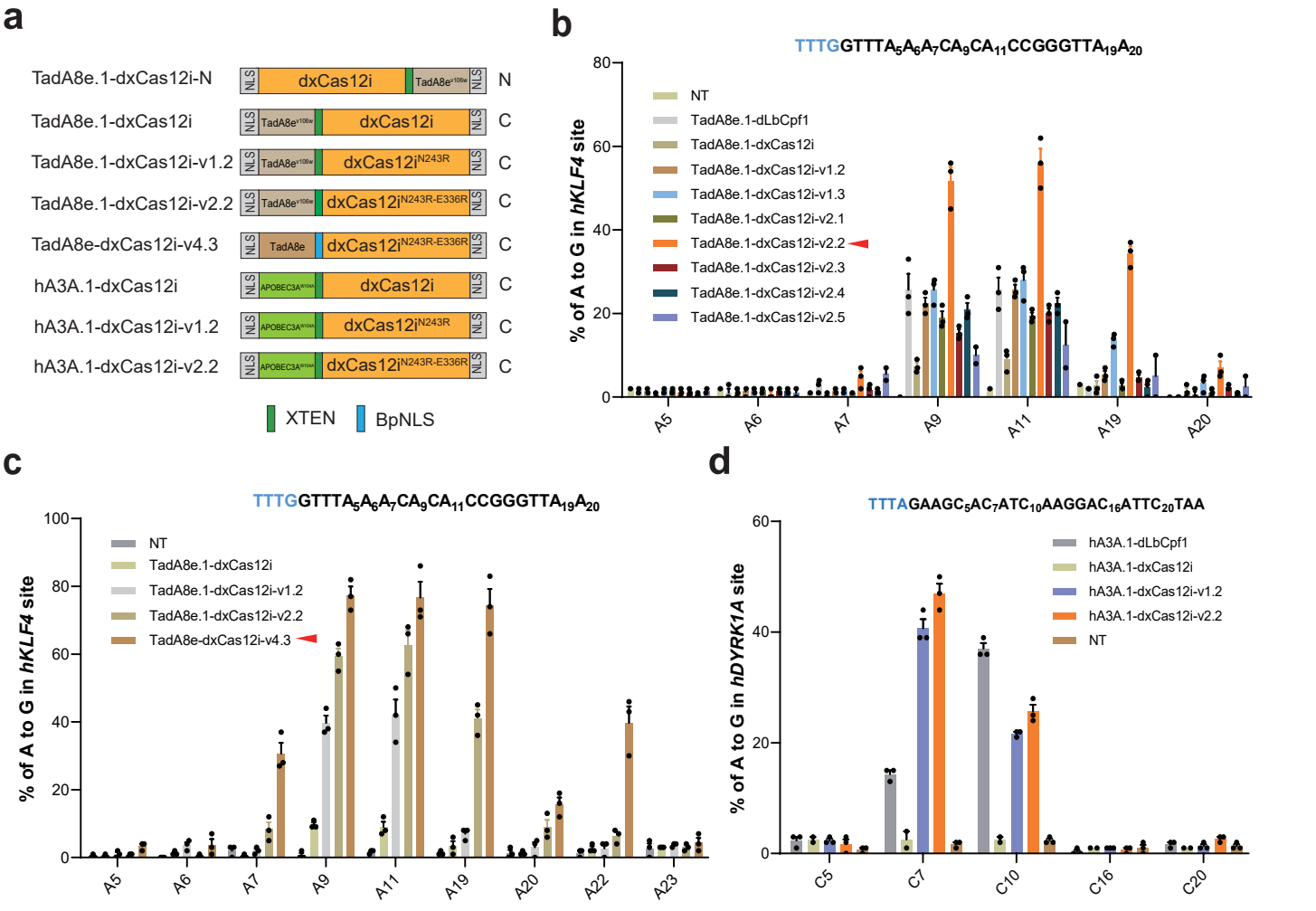

Fig.4 dCas12Max-TadA8e and dCas12Max-hA3A.1 mediated high base editing activity. **a**, Schematics of different versions of dCas12Max BEs. **b**, The A-to-G editing activity of TadA8e.1-dxCas12i-v2.2 was largely increased by combining v1.2 and v1.3 variant. **c**, Comparison of A-to-G editing frequency at the KLKF4 site from TadA8e.1-dxCas12i-v1.2, v2.2 and v4.3, ABE-dCas12Max (TadA8e-dxCas12i-v4.3) shows a high editing activity of 80%. **d**, Comparison of C-to-T editing frequency at the DYRK1A site from hA3A.1-dxCas12i, -v1.2 and v2.2, CBE-dCas12Max (hA3A.1-dxCas12i-v2.2) shows a high editing activity of 50%.

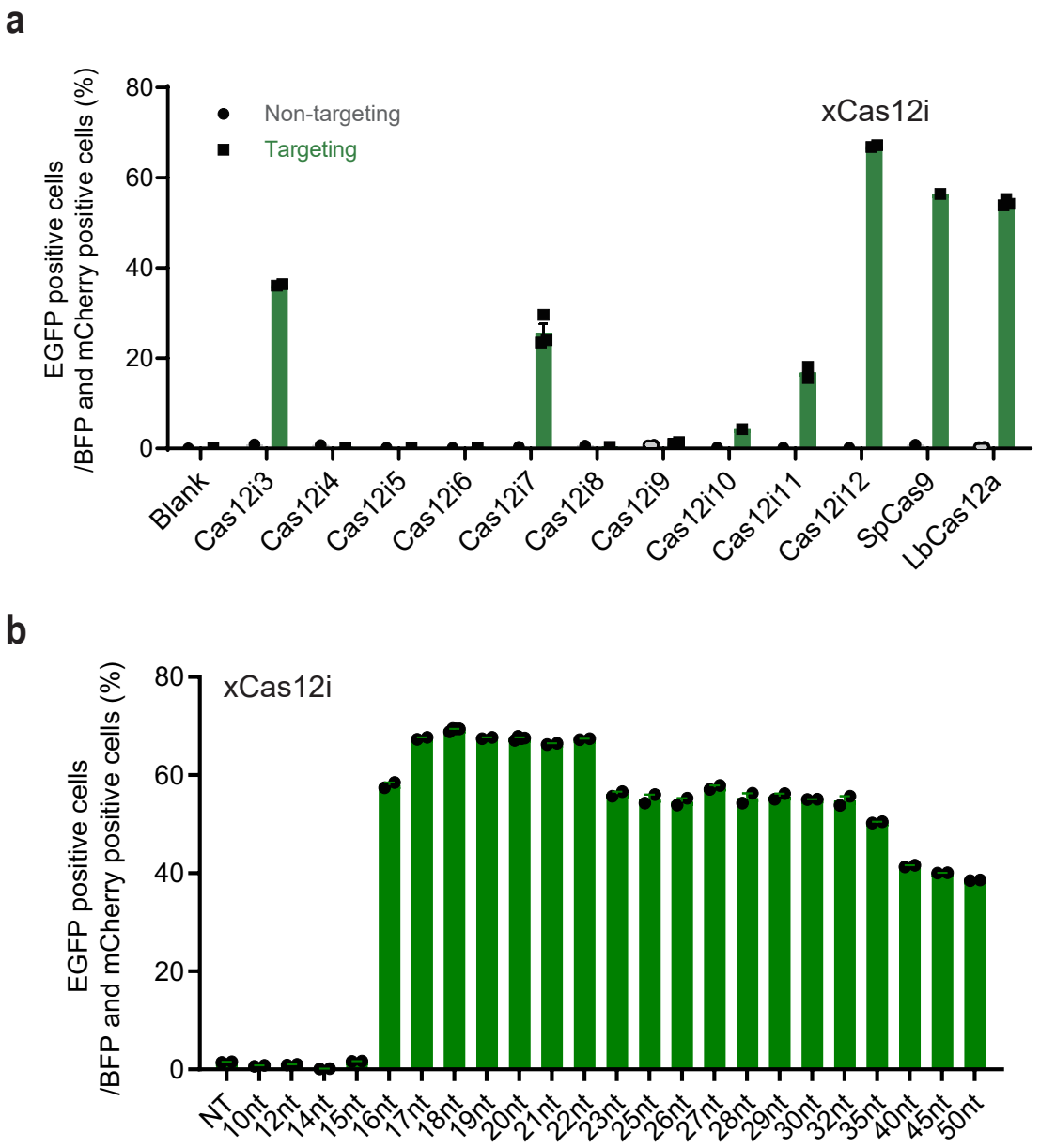

Supplementary Figure 1. Screen for functional Cas12i in HEK293T cells. a, Five of ten natural Cas12i nuclease mediate EGFP-activated efficiency in HEK293T cells. **b,** Optimal spacer length for xCas12i.

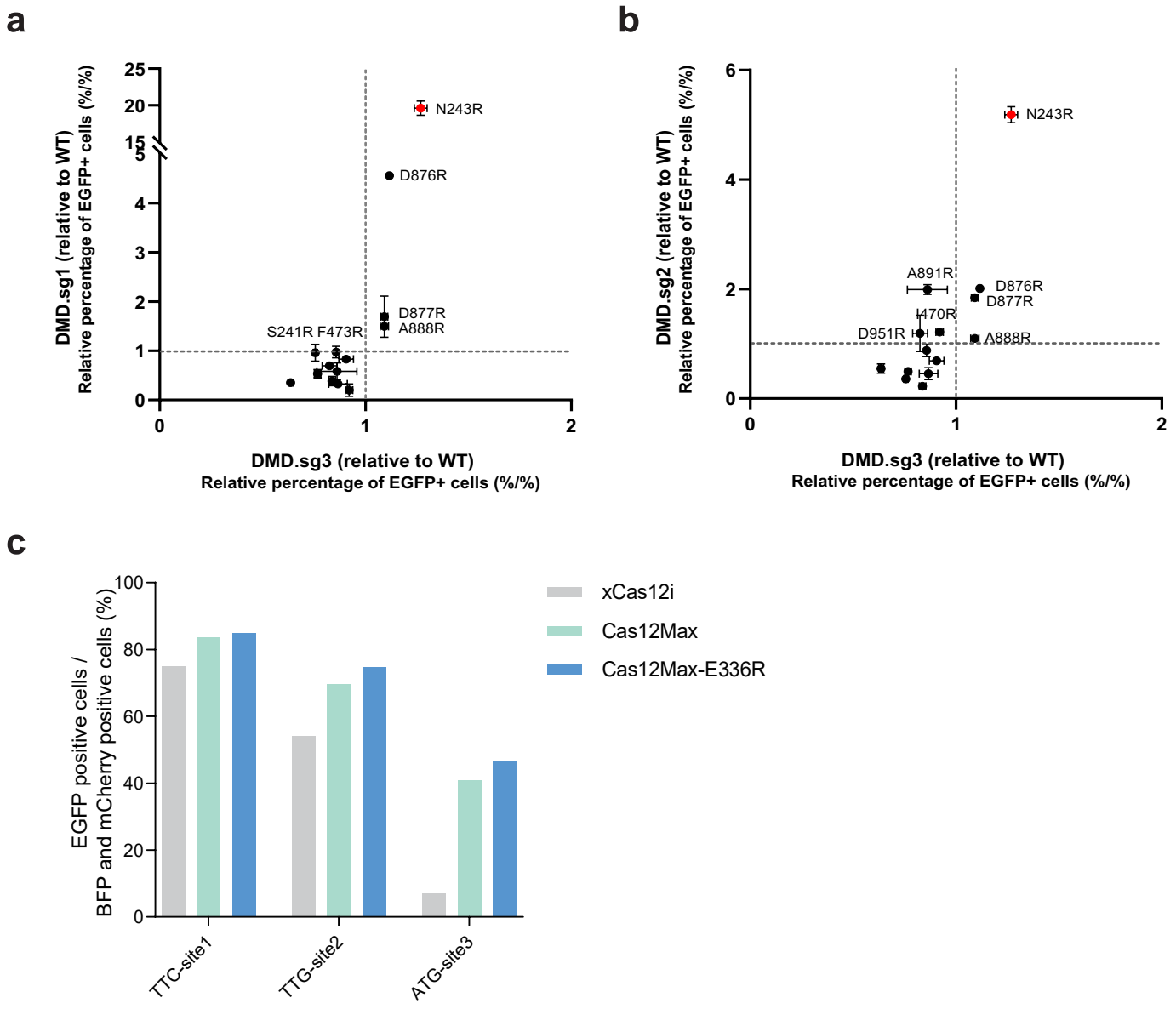

Supplementary Figure 2. Other mutants mediate high-efficiency editing. a-b, xCas12i mutant with N243R increased 1.2, 5, 20-fold activity at DMD.1, DMD.2 and DMD.3 locus. **c,** Both Cas12Max (xCas12i-N243R) and Cas12Max-E336R elevated EGFP-activiated fluorescent at different PAM recognition sites.

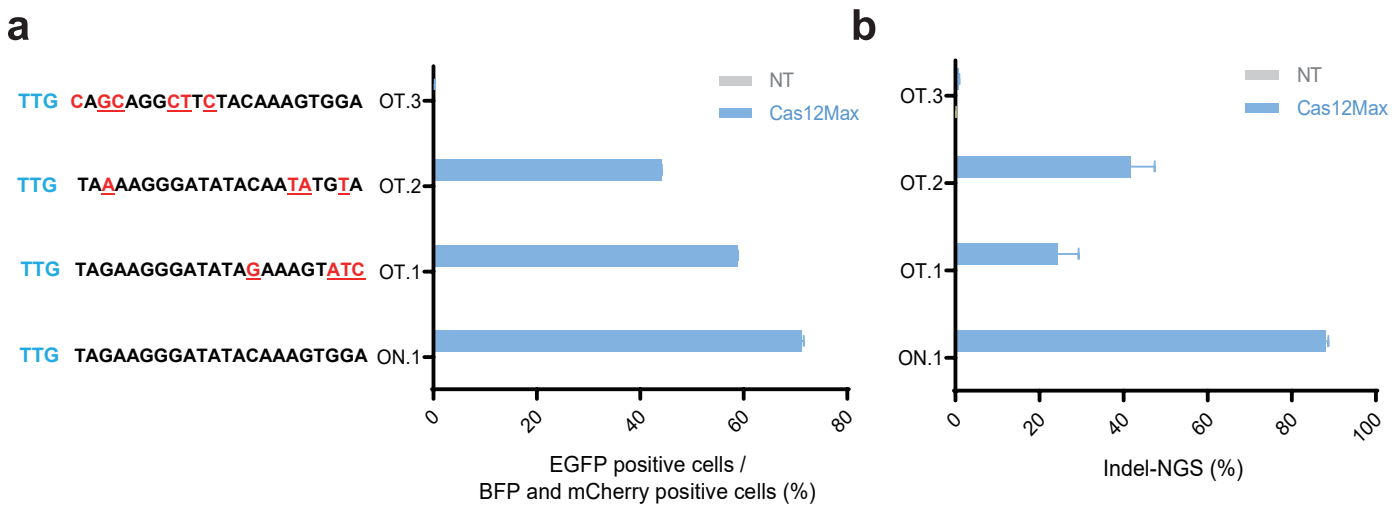

Supplementary Figure 3. Cas12Max induces off-target editing efficiency at sites with mismatches using the reporter system (a) and targeted deep sequence (b).

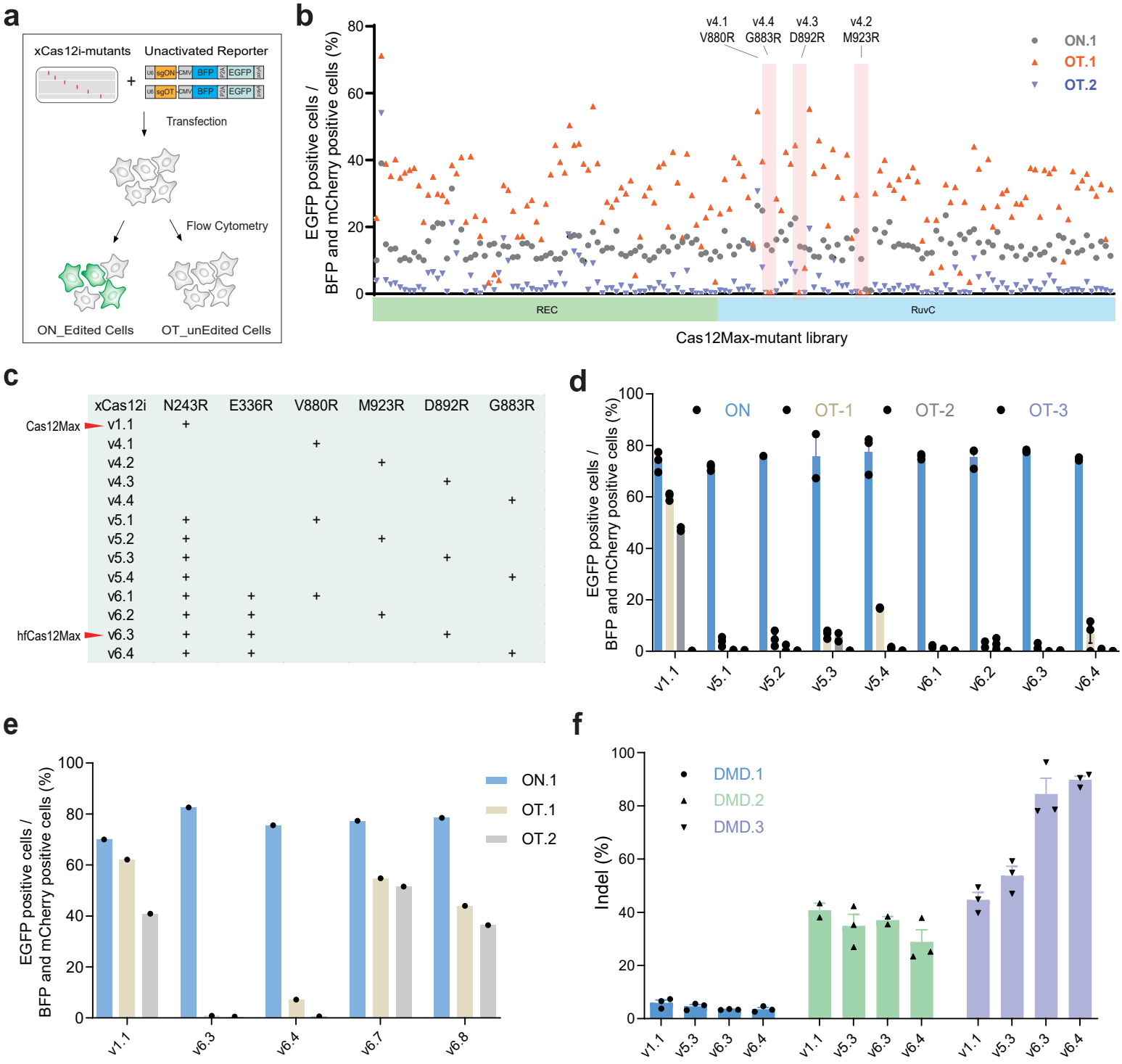

Supplementary Figure 4. hfCas12Max mediates high-efficiency and -specificity editing. a, Schematics of protein engineering stragetgy using unactivated EGFP reporter screening system with on-targeted and off-targeted crRNA. **b**, Rational protein engineering screen of over 200 mutants for highly-fidelity Cas12Max-.Four mutants show significantly decreased activity at both OT(off-target) sites and retains at ON.1 (on-target) site. **c**, Different versions of xCas12i. **d-e**, v6.3-hfCas12Max reduced off-target at OT.1 and OT.2 sites and and retained indel activity at TTR-ON targets, compared to v1.1-Cas12Max. **f**, v6.3-hfCas12Max retained comparable and higher activity at DMD.1, DMD.2, and DMD.3 locus, related to v1.1-Cas12Max.

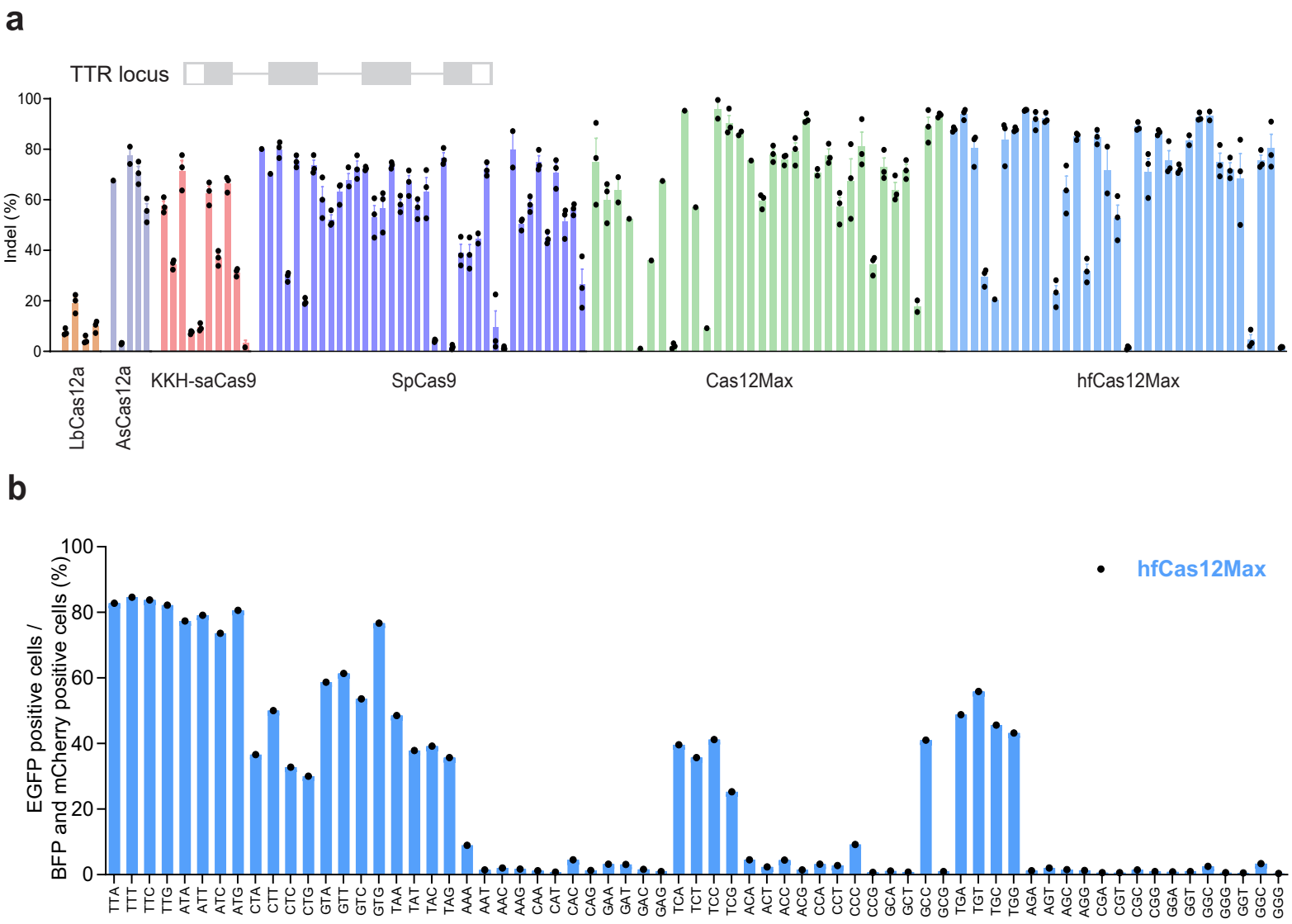

Supplementary Figure 5. hfCas12Max exhibited a broad PAM recognition and the high editing activity. **a**, Indel frenquencies from Cas12Max, hfCas12Max, LbCas12a, Ultra AsCas12a, SpCas9 and KKH-saCas9 at TTR locus. **b**, Cas12Max exhibits a broader PAM recognition profile with 5'TN- and 5'TNN- PAM.

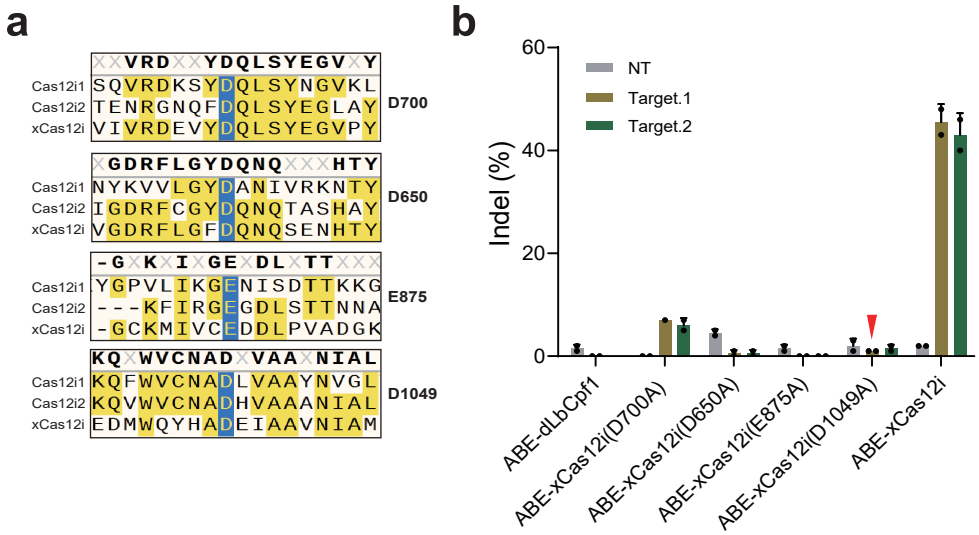

Supplementary Figure 6. Conserved cleavage sites of Cas12i. a, Sequence alignment of xCas12i, Cas12i1 and Cas12i2 shows that D650, D700, E875 and D1049 are conserved cleavage sites at RuvC domain. **b**, Introducing point mutations off D650A, E875A, and D1049A results in abolished activity of xCas12i.

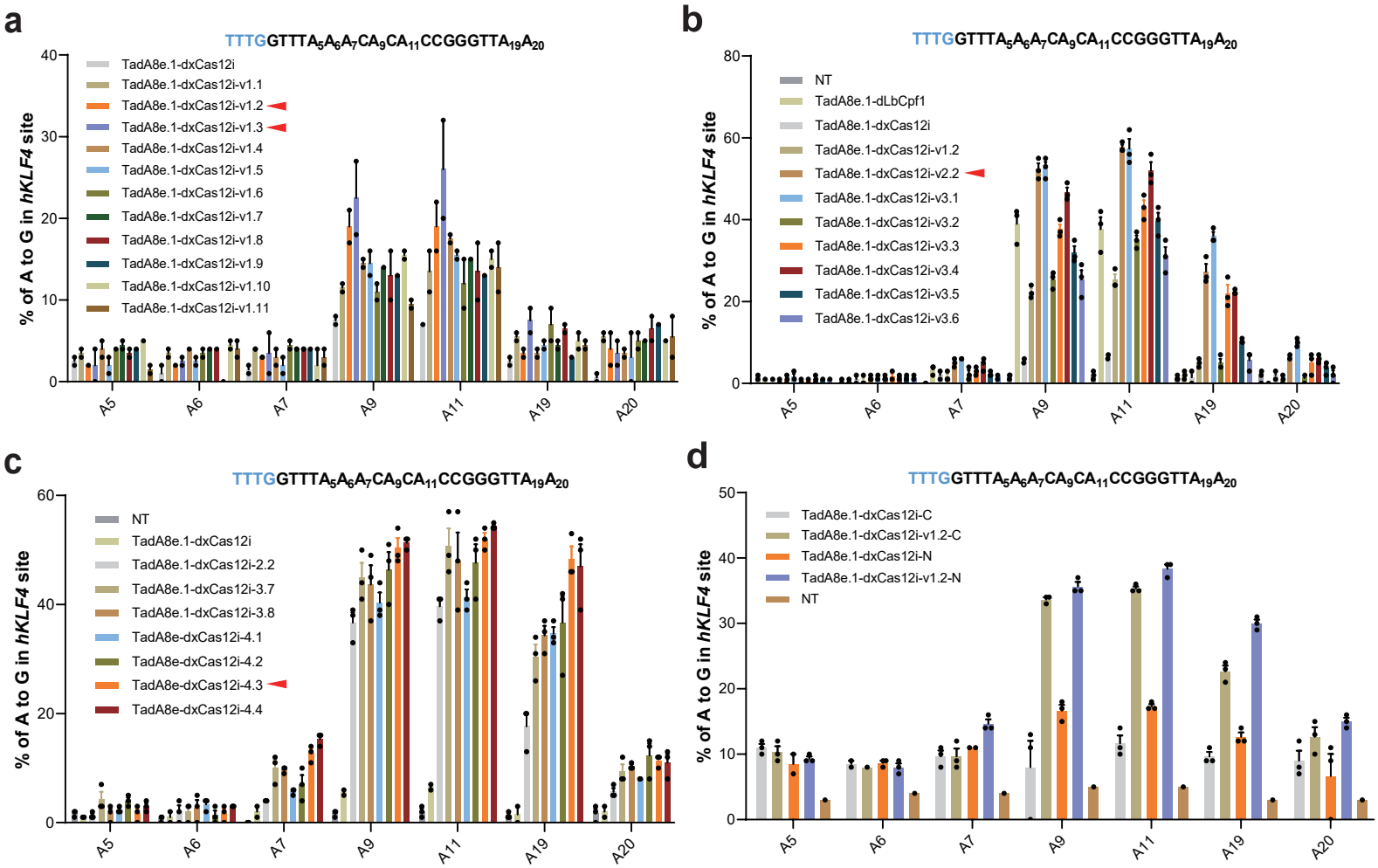

Supplementary Figure 7. Other strageties for high-efficiency ABE-dxCas12i. a, TadA8e.1-dxCas12i-v1.2 and v1.3 exhibits significantly increased A-to-G editing activity among various variants at KLKF4 site of genome. **b**, Unchanged or even decreased editing activity from various dCas12-ABEs carrying different NLS at N-terminal. **c**, Increased A-to-G editing activity of TadA8e-dxCas12i-v4.3 by combining v2.2, changed-NLS linker and high-activity Tade8e. **d**, dxCas12i-ABE-N by TadA at the C-terminus of dCas12 slightly increased editing activity.

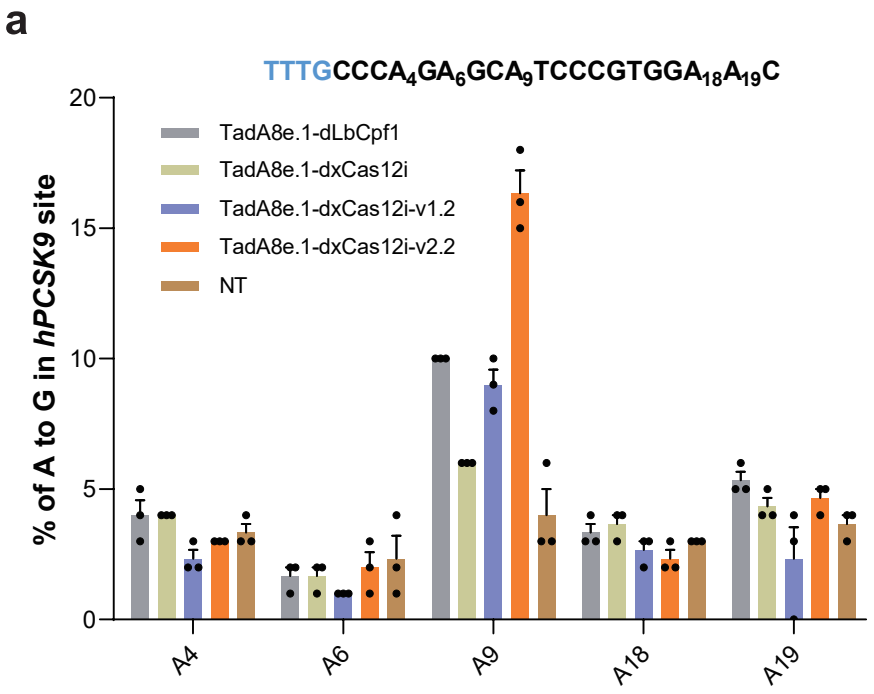

Supplementary Figure 8. Comparison of editing frequencies induced by various dCas12-BEs at different genomic target sites. a, Comparison of A-to-G editing frequencies induced by indicated TadA8e.1-dxCas12i, v1.2, v2.2, and TadA8e.1-dCas12a at PCSK9 genomic loucs.